MDAG.com Internet Case Study 51

A Case Study of Complex Drainage from an Acidic Waste-Rock Pile on a Marine Coast

by K.A. Morin

www.mdag.com/case_studies/cs51.html

TABLE OF CONTENTS

Abstract

This MDAG Case Study describes very complex and dynamic drainage from a highly acidic waste-rock pile on a marine coast. The drainage was complex both physically and geochemically. Iron staining and iron-encrusted layers on the foreshore confirmed submarine ARD discharge into the foreshore of the ocean that has relatively unlimited neutralizing capacity.

Drainage rates and directions changed twice daily due to tides, and seasonally due to wet and dry months of infiltration. Nevertheless, the overall average hydraulic gradient was roughly 0.001 towards the ocean. This was consistent with observed annual advances and retreats of chloride contours in groundwater between the waste-rock pile and the ocean.

Twice-daily tidal fluctuations of roughly 4 m were dampened inland by the waste rock and the underlying sand and gravel. As a result, inland groundwater-level fluctuations were roughly 1 m about 30 m inland from the shore, and about 0.1 m about 200 m from the shore.

Hydraulic conductivities (K) were estimated from the dampening of tidal fluctuations and from the time delays between peak tide levels and peak groundwater levels. The resulting K values for the waste rock were $1x10^{-2}$ to $8x10^{-2}$ m/s. This was about one to two orders of magnitude higher than K from single-well response (slug) tests performed under unreliable conditions. These high K values, combined with peak hydraulic gradients during tidal fluctuations, suggested turbulent (non-laminar) groundwater flow occurred in localized places and time.

Geochemically, three dynamic interfaces were defined: (1) the contact between fresh groundwater and seawater, (2) the contact between fresh groundwater and seasonally overlying ARD (a density inversion), and (3) the contact between ARD and underlying seawater at the foreshore that included substantial neutralization and secondary-mineral precipitation.

While simulations of this complex physical and geochemical drainage system would have been helpful and informative, modelling was not possible. There are no mathematical equations governing inverted three-density interfaces in very permeable materials with non-laminar flow in localized locations and with hourly and seasonally non-steady boundary conditions.

1. Introduction

Waste-rock piles have long been recognized as complex in three dimensions, with complex drainage time series (the fourth dimension) reflecting that complexity (e.g., the critical literature review of Morin et al., 1991; Morin and Hutt, 1997 and 2001; Morin, 2016 and 2017a and b). For piles releasing acidic drainage (ARD), the complexity increases due to density differences between the ARD and the "fresh" precipitation, groundwater, and/or stream water.

For acidic piles on marine coasts, the complexity of drainage is increased even further. This is primarily due to the presence of a third, strongly neutralizing water mass (seawater) with a third density range, driven cyclically into and from the waste rock by tidal fluctuations.

This MDAG Case Study 51 illustrates the dramatic physical and geochemical complexity of drainage from an acidic waste-rock pile on a marine coast.

2. General Description of The Coastal Waste-Rock Pile and Its Water Balance

This waste-rock pile was created primarily from washing waste from raw coal before shipping. Over roughly 70 years of operation, it grew from the marine shoreline out into the foreshore, filling the foreshore in places (Photo 2-1). The pile also contained a variety of other materials, like coke and building debris. Underlying sand and gravel represented the original land surface.

This coastal waste-rock pile covered approximately 13 hectares in lateral area, containing roughly one million cubic meters of waste. Recent erosion in places carried some waste into deeper marine areas. Elevations of pile ranged from 19 m above sea level to at least 2 m below sea level.

Due to the relatively coarse waste rock, little overland (surficial) flow occurred, and most precipitation infiltrated into the waste rock to become submarine-discharging groundwater. The water balance, based on monthly volumes of precipitation, suggested that groundwater infiltration through the pile could vary by a factor of almost 100 times from month to month. On average, an estimated 150,000 m^3/year of groundwater infiltration annually passed through the waste-rock pile, carrying inorganic contaminants.

Because this pile was on the shoreline, contaminated groundwater did not flow deep into the groundwater system. It remained shallow, with submarine discharge along the foreshore (discussed below in Section 3 along with Photos 3-1 and 3-2). The interaction of this groundwater flow with the foreshore was complex, as the following sections illustrate.

There were three groundwater masses in and beneath the waste-coal pile: lowest-density background groundwater, medium-density ARD from the waste rock, and highest-density seawater (discussed below in Section 4.4 and Figure 4-6).

Photo 2-1. Air photograph of the coastal waste-rock pile.

3. Description of Acidic Drainage Chemistry from This Pile

Geochemical information on the inorganic contamination from this pile was based on several one-time "static" and repetitive "kinetic" geochemical tests. Static acid-base accounting (ABA), showed elevated, potentially acid-generating sulphide was present in most samples, and most samples were acidic.

Two laboratory-based humidity cells were operated for 26 weeks, with samples being leached weekly to identify geochemical leaching patterns. Weekly effluent pH generally decreased after the initial week, then generally stabilized around pH 1.8 to 2.2. Compared to the worldwide International Kinetic Database[1], pH from these two cells was among the lowest measured in many hundreds of humidity cells from around the world.

Mean acid rock drainage (ARD) from this waste-rock pile had a pH around 2.2 with a conductivity of nearly 4000 µS/cm, sulphate around 2600 mg/L, acidity to pH 8.3 around 2900 mg/L, and iron nearly 600 mg/L. In the maximum case, aluminum and iron approached or exceeded 1000 mg/L.

Because this waste-rock pile drained primarily into the ocean with a relatively unlimited neutralizing capacity, all ARD entering the ocean was neutralized. This neutralization was marked by substantial secondary-mineral precipitation including rusty-coloured iron oxyhydroxides. During low tide, prominent iron staining could be seen on the foreshore (Photos 3-1 and 3-2), marking submarine discharge of the ARD into the ocean. Additionally, parallel sediment layers, dipping seaward, of hard geochemical iron "cement" (ferricrete) were seen sub-parallel to the shoreline (Photos 3-3 and 3-4). These were interpreted as past, relatively stable interfaces between the waste rock and the ocean (and between ARD and neutralizing ocean water), before waste rock was progressively eroded inland.

[1] http://www.mdag.com/ikd.html

Photo 3-1. Heavily iron-stained foreshore due to ARD neutralization, exposed at low tide.

Photo 3-2. Closeup of Photo 3-1.

Photo 3-3. Parallel layers, dipping seaward, of hard geochemical iron "cement" (ferricrete), apparently representing past, relatively stable interfaces between the waste rock and the ocean (and between ARD and neutralizing seawater).

Photo 3-4. Closeup of Photo 3-3.

4. Complex Drainage from This Waste-Rock Pile

4.1 General Description of Drainage

Regular tidal fluctuations at this location were -2 m to +2 m relative to mean tide level. In comparison, many groundwater elevations ranged from slightly below mean tide level to +1 m above. This suggested a well-drained groundwater system with low hydraulic gradients, consistent with relatively coarse waste rock, but with a significant potential for tidal effects.

Although tidal ranges were typically around 4 m, groundwater elevations close to the shoreline displayed short-term fluctuations of up to about 1 m. Groundwater levels in the set of monitor wells collected over more than several minutes to an hour could not be reliably compared, because of tidal-caused fluctuations during the data-collection period. Nevertheless, the temporal mean net hydraulic gradient was roughly estimated at 0.001 outwards towards the ocean.

These groundwater levels generally incorporated the concept of freshwater-equivalent head, although it was more complicated for this site. Variable densities of the groundwater through time and location (discussed further in Section 4.4) meant that groundwater levels even in each well were not necessarily directly comparable.

Groundwater elevations in each monitor well showed that there were seasonal trends. The six wetter months generally corresponded to higher water-table elevations, which was consistent with expectations from the general water balance in a relatively fast drainage system. However, the net effect of this seasonal variation combined with twice-daily tidal variations was complex (Section 4.2).

This trend of seasonal infiltration was also consistent with aqueous chloride concentrations at selected monitor wells and other sampling sites, but there was additional complexity. Relative to local seawater with approximately 12,000 mg/L of chloride, the groundwater chloride contour of 10,000 mg/L was progressively pushed outward during wetter months, from several tens of meters inland under the waste-rock pile, out to tens of meters beneath the ocean. Thus, the increased infiltration and higher elevations of groundwater during the wetter months apparently forced the freshwater-seawater interface temporarily seaward (discussed further in Section 4.4).

However, the 1,000 mg/L chloride contour migrated outwards only approximately to the shoreline. Moreover, the 100 mg/L contour remained relatively stationary beneath the pile during all monitoring events. Overall, this suggested the mass of non-seawater-diluted water (upgradient groundwater and/or acid rock drainage) remained roughly 50 m inland, while the mixing zone with seawater varied from inland to offshore as infiltration varied (Interfaces 1 and 3 discussed in Section 4.4).

4.2 Influence of Tides on Groundwater Levels

Maximum tidal amplitude, one-half the range, was approximately 2 m, occurring as semi-diurnal (two tide cycles a day) and mixed (the two daily tide cycles with different amplitudes). The corresponding amplitudes for Monitor Wells MW1 (~30 m from the shoreline in the waste-coal pile), MW2, and MW3 (in the center of the waste-rock pile) decreased with their increasing distances from the nearest shoreline (Table 4-1). Based on this, a generalized schematic of the water table is shown in Figure 4-1, assuming constant density. The delays between high tide and high groundwater level increased with increasing distance, as did the delays between low tide and low groundwater level, but not proportionally and not to the same degree. This is discussed further in the following subsection.

Table 4-1. Effect of Tidal Fluctuation on Groundwater Levels Beneath the Waste-Rock Pile

Characteristic	Tide	Monitor Well MW1	Monitor Well MW2	Monitor Well MW3
Approximate Distance from Nearest Shoreline (m)	0	30	80	200
Approximate Range from Lowest to Highest Tide (m)	4	0.8-1.1	0.1-0.3	0.05-0.10
Approximate Time Delay from High Tide to High Groundwater Level (hours)[1]	0	0.25-0.5	3-4	3-5
Approximate Time Delay from Low Tide to Low Groundwater Level (hours)	0	2-3	5-7	6-8

[1] The delay time was greater for the higher high tide than the lower high tide at MW2, and the response to the higher high tide was not observed at MW3; the higher high tide during a day in a wet month created faster response and much shorter delay times at MW2 and MW3, suggesting an overlying, more permeable layer had been reached.

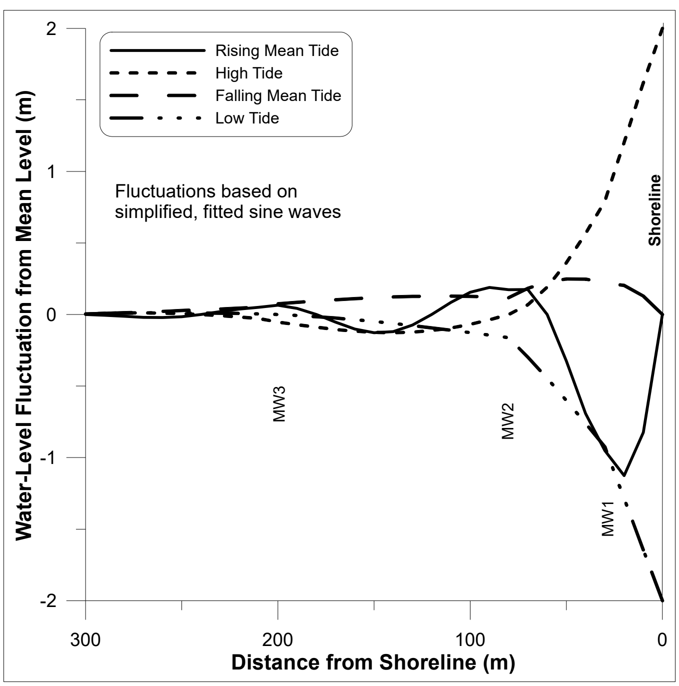

Figure 4-1. Fluctuations of groundwater levels due to tides; one-dimensional trends with distance from the shoreline for three monitor wells.

Much shorter delays at MW2 and MW3 for the higher high tide during a day in a wet month suggested a more permeable overlying layer in the waste rock was reached as the groundwater levels increased. This is consistent with the discussion in the next paragraph.

At MW1 about 30 m inland and at MW2 about 80 m inland, the higher high tide of the day produced a similar or lower groundwater level than the lower high tide. This was interpreted as high-tide water rushing inland, but the higher high-tide water being attenuated by an unsaturated zone in the underlying lower-K material (Figure 4-2; see also low-tide and rising-mean line in the top of Figure 4-1). This also explained the observed "tailing" effect at MW1. In MW1, the slower drainage from the deeper, now-saturated, lower-K layer was more gradual and drawn out in response to the lower low tide relative to the subsequent rise.

At MW3 ~200 m inland, groundwater fluctuations showed only a 12-hour diurnal variation, rather than the tidal semi-diurnal 6-hour variation. This response at MW3 could be due to (1) smoothing of the water-table fluctuations, and/or (2) superposition of tidal fluctuations arriving at MW3 at different times (e.g., lateral anisotropy) from a roughly 180-degree circular waste-rock circumference exposed to tides (Photo 2-1).

4.3 Hydraulic Conductivities of Subsurface Layers

Saturated hydraulic conductivity (K) is typically defined as the ease with which groundwater flows through a unit volume of material under standardized conditions. K is partly dependent on the fluid passing through the material. Because fresh water, acid rock drainage, and seawater were all present beneath the waste-rock pile, the estimation of K became complex (the three masses of water are discussed further in Section 4.4).

Hydraulic conductivity (K) was estimated from single-well response ("slug") tests. The well screens typically crossed more than one lithology and the prescribed boundary conditions for slug tests were often not met. Nevertheless, K in the waste rock was estimated as roughly 10^{-3} to 10^{-4} m/s, whereas the underlying sand and gravel was measured at $6x10^{-5}$ to $9x10^{-5}$ m/s.

As explained above and in Table 4-1, three monitor wells showed subdued and delayed responses to mixed, semi-diurnal tidal fluctuations. These fluctuations migrated into the waste-rock pile from approximately 180 degrees of its circumference. Equations exist to roughly estimate K from the subdued ("dampened") monitor-well responses and the delayed responses, leading to values listed in Table 4-2.

As a result, the tidal-damping method applied to waste rock yielded a K range of $1x10^{-2}$ to 8×10^{-2} m/s (Table 4-2), which was higher than 10^{-3} to 10^{-4} m/s from slug tests. The tidal-delay methods applied to the underlying sand and gravel yielded a range of K from $1x10^{-5}$ to $4x10^{-4}$ m/s, consistent with 6-9 x 10^{-5} m/s from slug tests. The tidal-delay values ignored some higher high tides, where delay times were much shorter, suggesting a more permeable overlying layer was reached.

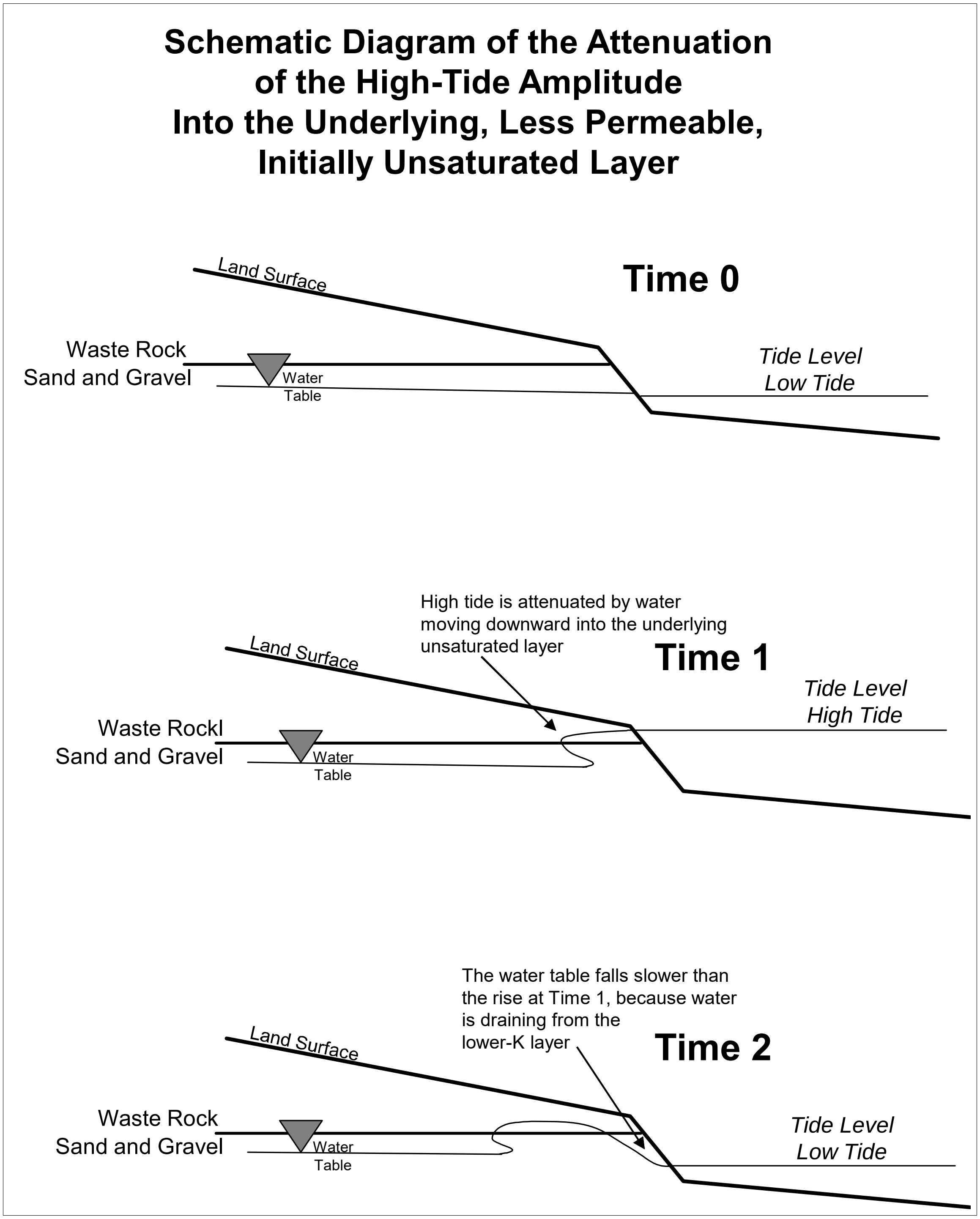

Figure 4-2. Schematic diagram for the attenuation of high-tide amplitude by an underlying unsaturated layer.

Table 4-2. Calculated Hydraulic Conductivities Based on Monitor-Well Responses to Tidal Fluctuations[1]

Hydraulic Conductivity (m/s)[2]	Monitor Well MW1	Monitor Well MW2	Monitor Well Mw3
Tidal Damping Method	$1x10^{-2}$	$2x10^{-2}$	$8x10^{-2}$
Tidal Delay Method using High Tide	$4x10^{-4}$	$5x10^{-5}$	$2x10^{-4}$
Tidal Delay Method using Low Tide	$1x10^{-5}$	$1x10^{-5}$	$6x10^{-5}$

[1] Based on data in Table 4-1 and reconciled equations in Millham and Howes (1995).

[2] Calculated from transmissivity (m^2/s) and an assumed saturated thickness of 1 m for the conductive layer; see text for discussion and for other values of saturated thickness.

The K values based on the damping and the low-tide delay methods increased as the distance inland increased. Because K was calculated from T based on an assumed consistent saturated thickness of 1 m, this could be alternatively explained by a narrowing of the conductive, saturated flow thickness towards the shoreline.

Based on Table 4-2 and the assumption of a constant waste-rock K, the equivalent conductive saturated thickness could be roughly 6-8 m at MW3 (~200 m from shoreline), narrowing to 1-2 m at MW2 (~80 m from shoreline), and to 1 m at MW1 (~30 m from shoreline). This was based on the Tidal Damping and Low-Tide Tidal Delay Methods, but not on the High-Tide Tidal Delay Method due to the complexity depicted in Figure 4-2.

4.4 Subsurface Interfaces of Three Density-Distinct Migrating Water Masses

One major complexity in the movement of groundwater beneath this waste-rock pile is the interface between seawater and the less dilute "freshwater". In its simplest form, the interface is considered a sharp, vertically sloping boundary with no water movement. This leads to the century-old Ghyben-Herzberg relationship. For every meter of freshwater height above ocean level, the interface lies at least 40 m below ocean level. This is shown in Figure 4-3, for both freshwater with a theoretical density of 1000 kg/m^3, and for acid rock drainage from the waste-rock pile with an approximate density of 1010 kg/m^3, compared with seawater at 1025 kg/m^3. The ARD is more dense, so it would "push" the interface deeper into the underlying sand and gravel, but there were no deep monitor wells to confirm this.

Figure 4-3 is a gross simplification. In reality, there is some movement along the interface. Freshwater is forced upwards along the interface by upgradient groundwater, and as a result some seawater is recirculated back to the sea (Figure 4-4). This creates a mixing zone of the two waters. Figure 4-4 also shows more complex scenarios, where some seawater forms a lens above freshwater. This lens is consistent with Figure 4-2 for this waste-rock site, but cannot be mathematically described or simulated (Post et al., 2007).

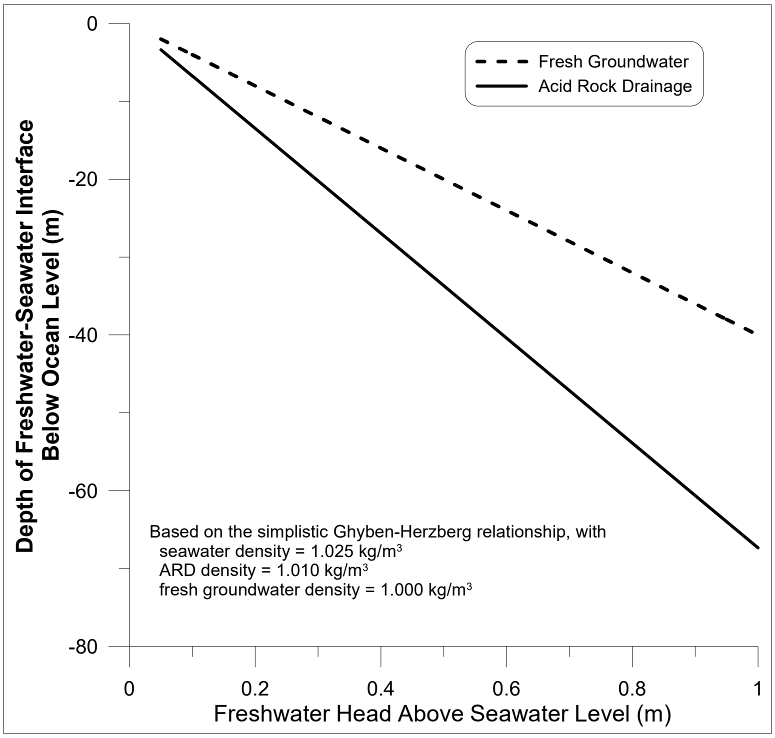

Figure 4-3. Depth of the freshwater-seawater interface relative to freshwater head above seawater, for fresh (dilute) groundwater (dashed line) and local acid rock drainage (solid line).

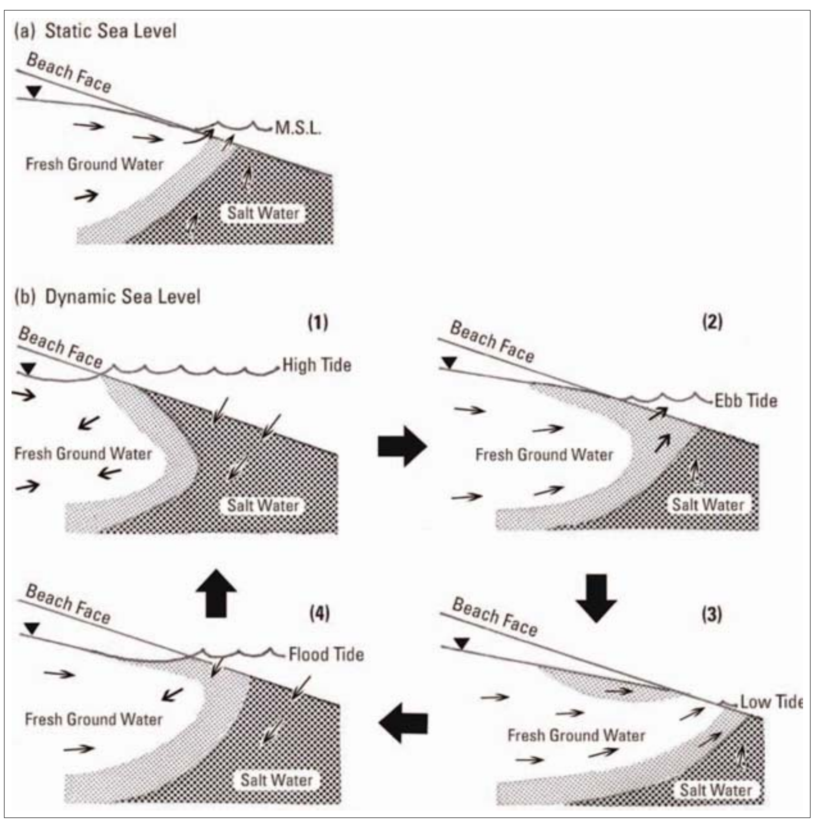

Figure 4-4. An example of a more realistic freshwater-seawater interface (from Urish and Ozbilgin, 1989).

Nevertheless, even Figure 4-4 does not fully capture the complexity here. Unlike Figure 4-4 which shows a two-density interface, drainage from this waste-rock pile has waters of three densities (Figure 4-5) with three interfaces (Figure 4-6).

The upgradient, lowest-density groundwater moves beneath the waste-rock pile and encounters highest-density seawater, and creates Interface 1 similar to Figure 4-4. However, the middle-density ARD, which is highly variable monthly, moves downward through the pile and seasonally creates two more interfaces (Figure 4-6). Interface 2 lies between the ARD and upgradient groundwater, whereas the ARD and seawater create Interface 3.

It would be helpful and informative to simulate the complex, non-steady (hourly and seasonally), dynamic scenario of Figure 4-6. This is not possible for several reasons.

- Most groundwater models are based on principles like Darcy's Law and fluid continuity under laminar flow. However, calculations of the Reynold's Number for this waste-rock pile suggest groundwater flow became turbulent at the higher values of hydraulic conductivity and at higher hydraulic gradients during peak tidal fluctuations.

- Furthermore, Guo and Langevin (2002) highlighted the problems of simulating saltwater-freshwater in a dynamic groundwater system not in equilibrium (including the density inversion at Interface 2).

- There are also mathematical issues with the highly variable boundary conditions in time and space (Robinson and Gallagher, 1999).

- Finally, there are no mathematical equations governing inverted three-density interfaces in very permeable materials with non-laminar flow in localized locations and with hourly and seasonally non-steady boundary conditions.

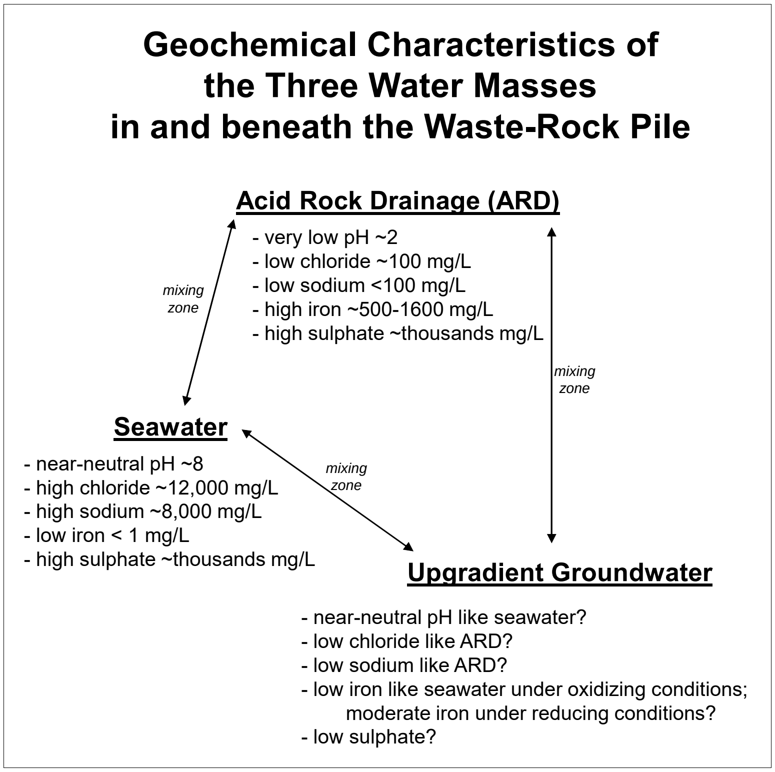

Figure 4-5. Geochemical characteristics of the three water masses in and beneath this waste-rock pile.

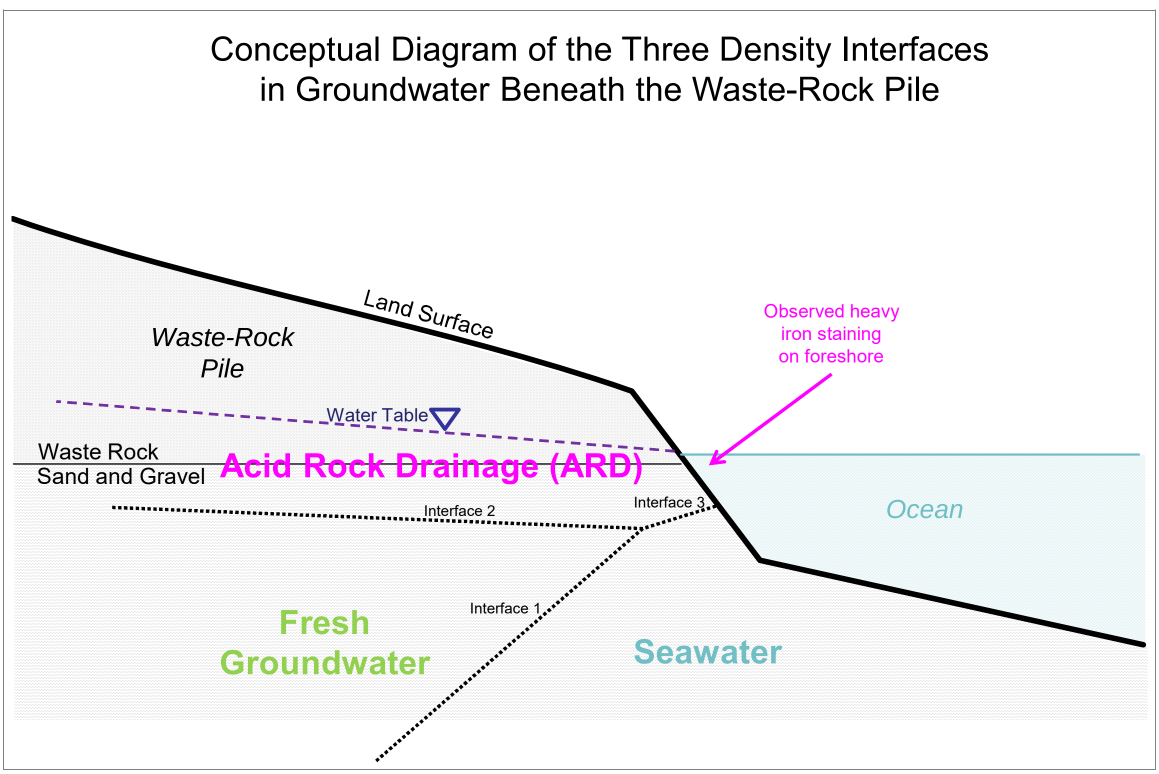

Figure 4-6. Schematic diagram of the three geochemical interfaces beneath this waste-rock pile (see Photos 3-1 and 3-2 for the foreshore iron staining).

5. References

Guo, W., and C.D. Langevin. 2002. User's Guide to SEAWAT: A Computer Program For Simulation of Three-Dimensional Variable-Density Ground-Water Flow. U.S. Geological Survey Open-File Report 01-434.

Millham, N.P., and B. L. Howes. 1995. A comparison of methods to determine K in a shallow coastal aquifer. Ground Water, 33, p. 49-57.

Morin, K.A. 2017a. A Case Study of Rapid Water Flow through Full-Scale Waste-Rock Piles. MDAG Internet Case Study #45, www.mdag.com/case_studies/cs45.html

Morin, K.A. 2017b. A Case Study of High-Frequency Time Series for Individual Chemical Elements in Waste-Rock Drainage. MDAG Internet Case Study #46, www.mdag.com/case_studies/cs46.html

Morin, K.A. 2016. Spectral Analysis of Drainage from Highly Reactive Geologic Materials. ISBN 978-0-9952149-1-0. Free e-book at www.MDAG.com/spectral-book.html

Morin, K.A., and N.M. Hutt. 2001. Environmental Geochemistry of Minesite Drainage: Practical Theory and Case Studies, Digital Edition. MDAG Publishing (www.mdag.com), Surrey, British Columbia. ISBN: 0-9682039-1-4.

Morin, K.A., and N.M. Hutt. 1997. Environmental Geochemistry of Minesite Drainage: Practical Theory and Case Studies. MDAG Publishing (www.mdag.com), Surrey, British Columbia. ISBN: 0-9682039-0-6.

Morin, K.A., E. Gerencher, C.E. Jones, and D.E. Konasewich. 1991. Critical Literature Review of Acid Drainage from Waste Rock. MEND Report 1.11.1.

Post, V., H. Kooi, and C. Simmons. 2007. Using hydraulic head measurements in variable-density ground water flow analyses. Ground Water, 45, p. 664-671.

Robinson, M.A., and D.L. Gallagher. 1999. A model of groundwater discharge from an unconfined coastal aquifer. Ground Water, 37, p. 80-87.

Urish, D.W., and M.M. Ozbilgin. 1989. The coastal ground-water boundary. Ground Water, 27, p. 310-315.